n_{i0}	characteristic constant for each family of substances
α_i	molecular polarizability of the component i, $cm^3\ mol^{-1}$
a_j	polynomial coefficients in eq 4
n_A, n_D	refractive indexes of A and D in eq 6
φ_A	volume fraction of the component A in eq 6
n	polynomial degree
ρ	density of the solution, g cm^{-3}

Registry No. Methyl isobutyl ketone, 108-10-1; *sec*-butyl alcohol, 78-92-2; isobutyl alcohol, 78-83-1; *n*-butyl alcohol, 71-36-3.

Literature Cited

(1) Gopalakrishnan, R. *J. Prakt. Chem.* **1971**, *6*, 1178.
(2) Riggio, R.; Ramos, J. F.; Hernandez Ubeda, M.; Espíndola, J. A. *Can. J. Chem.* **1981**, *59*, 3305.
(3) Kirkwood, J. G. *Phys. Z.* **1931**, *33*, 57.
(4) Sôlimo, H. N.; Alonso, S. del V.; Katz, M. *Can. J. Chem.* **1979**, *57*, 768.
(5) Boyer-Donzelot, M. Doctoral Thesis, University of Nancy I, Nancy, France, 1974.
(6) Boyer-Donzelot, M.; Barriol, J. *Bull. Soc. Chim. Fr.* **1973**, *11*, 2972.
(7) Robertson, G. R. *Ind. Eng. Chem., Anal. Ed.* **1939**, *11*, 464.
(8) Radi, H. S. *J. Phys. Chem.* **1973**, *77*, 424.
(9) Riddick, J. A.; Bunge, W. B. "Organic Solvents", 3rd ed.; Wiley-Interscience: New York, 1970; Vol. II.
(10) Weast, J. "Handbook of Chemistry and Physics", 58th ed.; CRC Press: Cleveland, OH, 1977.
(11) Voronkov, M. G.; Deich, A. Y. *Teor. Eksper. Khim., Akad., Nauk. Ukr. SSR.* (*Engl. Transl.*) **1965**, *1*, 443.
(12) Voronkov, M. G.; Deich, A. Y.; Akatova, E. V. *Khim. Geterotsikl. Soedin., Akad. Nauk. Lat. SSR.* (*Engl. Transl.*) **1966**, *2*, 5.

Received for review May 6, 1982. Revised manuscript received March 22, 1983. Accepted April 7, 1983. Support of this research by the INENCO of the Universidad Nacional de Salta-República Argentina is greatly appreciated.

Thermodynamic Properties of Isobutane in the Critical Region

J. M. H. Levelt Sengers,[*†] **B. Kamgar-Parsi,**[‡] **and J. V. Sengers**[†‡]

Thermophysics Division, National Bureau of Standards, Washington, D.C. 20234, and Institute for Physical Science and Technology, University of Maryland, College Park, Maryland 20742

For geothermal applications, a scaled fundamental equation has been formulated in order to represent and tabulate the thermodynamic properties of isobutane in the critical region. In the supercritical range, the surface joins smoothly with that of Waxman and Gallagher, to which it is a complement. The range of the surface is 405–438 K in temperature, 150–290 kg/m^3 in density. The critical constants are T_c = 407.84 ± 0.02 K, ρ_c = 225.5 ± 2 kg/m^3, P_c = 3.629 ± 0.002 MPa. Comparisons are made with the *PVT* data of Beattie et al., and of Waxman, and also with the formulations of Waxman and Gallagher, and of Goodwin and Haynes.

Introduction

Isobutane has been proposed as the working fluid in binary geothermal power cycles. In this application, the fluid would pass through the heat exchanger at a pressure exceeding the critical pressure (P_c = 3.63 MPa), while it is heated from ambient to supercritical temperatures (T_c = 408 K). The initial state of the fluid entering the turbine would be a supercritical pressure and temperature, while the density would be somewhat below the critical. The gas would then expand isentropically along a path that, preferably, should remain within the one-phase vapor region. Kestin and Khalifa (*1*, *2*) pointed out that the then-existing formulations of the thermodynamic properties of isobutane were of insufficient reliability for design of an efficient cycle. The lack of reliability was due, to a considerable extent, to sparsity and inconsistency of the thermodynamic data. Since then, the situation has been remedied, at least to a good extent, by the acquisition of new data on the vapor pressure and on *PVT* of the vapor and supercritical phase by Waxman et al. (*3*–*6*), and on *PVT* of the liquid by Haynes (*7*). These new accurate data permitted Waxman et al. to select the bodies of reliable data.

It was decided to approach the formulation of the thermodynamic surface in two steps. Waxman and Gallagher (*5*, *6*) adapted the free energy model developed by Haar and coworkers (*8*) to represent the thermodynamic properties of isobutane up to 40 MPa and from 250 to 700 K with the exclusion of a region around the critical point the size of which is

$$0.985 \le T_c/T \le 1.015 \qquad \text{i.e., } 401.8 \le T \le 414 \text{ K}$$

$$0.7 \le \rho_c/\rho \le 1.3 \qquad \text{i.e., } 173.4 \le \rho \le 322 \text{ kg/m}^3 \tag{1}$$

The thermodynamic surface that we present here is valid in the range

$$405 \le T \le 438 \text{ K}$$

$$150 \le \rho \le 290 \text{ kg/m}^3 \tag{2}$$

and thus supplements the surface of Waxman et al. in most of the excluded range. The model that we use is that of revised and extended scaling, as developed according to the modern theory of critical phenomena (*9*). We have applied this model successfully to the thermodynamic properties of light and heavy water (*10*, *11*) in the critical region. Here, however, we use a somewhat different approach toward determining the model parameters. We obtained most of our parameter values by a fit to the experimental *PVT* data of Beattie et al. (*12*, *13*), which were recently validated by Waxman (*6*). There are a large number of *PVT* data in a very narrow temperature region, from 407.8 to 408.3 K, around the critical point; the only other data available in our range are on the 423.17 K isotherm. It is clear that temperature derivatives of the surface cannot be reliably taken if the surface is based on only two isotherms. We therefore supplemented the experimental data with *PVT* points generated from the surface of Waxman et al. in a range in which the surface is valid. This practice has yielded three benefits. It has helped pinpoint our surface, has ensured a smooth crossover to the analytic surface along most of the boundary, and has provided the entire analytic "background" for the caloric parameters, for which, in the case of isobutane, no experimental information is available.

The critical-point parameters incorporated in the scaled equation differ from those reported by Beattie et al. (*12*). If the critical parameters are freely adjusted in the fit to a scaled equation, the value of the critical temperature falls as much as

---

[†] National Bureau of Standards.

[‡] University of Maryland.

0.3 K below that deduced by Beattie et al. from the same data. An independent experimental determination of the critical temperature of isobutane by one of us (J.M.H.L.S.) gave results very close to the low value of T_c that we deduced from Beattie's data. This is the value that we then used in the fit.

We present here tabulated values derived from our fundamental equation for the saturation properties and for pressure, energy, enthalpy, entropy, specific heats at constant pressure and volume, and speed of sound, along isotherms in the range given by eq 2.

Comparisons are presented with the experimental *PVT* data, with the analytic surface of Waxman et al., and with the coexistence curve of Goodwin and Haynes (*7*).

Scaled Fundamental Equation

Our fundamental equation involves a relationship between the intensive thermodynamic variables pressure P, chemical potential μ, and temperature T. Specifically we consider the reduced variables

$$\tilde{P} = \frac{P}{T}\frac{T_c}{P_c} \qquad \tilde{\mu} = \frac{\mu}{T}\frac{\rho_c T_c}{P_c} \qquad \tilde{T} = -T_c/T \tag{3}$$

where P_c is the critical pressure, T_c the critical temperature, and ρ_c the critical density. The fundamental equation yields the thermodynamic potential $\tilde{P}$ as a function of $\tilde{\mu}$ and $\tilde{T}$ and has the form

$$\tilde{P} = \tilde{P}_0(T) + \Delta\tilde{\mu} + \tilde{P}_{11}\Delta\tilde{\mu}\Delta\tilde{T} + \Delta\tilde{P} \tag{4}$$

with

$$\Delta\tilde{T} = \tilde{T} + 1 \tag{5}$$

$$\Delta\tilde{\mu} = \tilde{\mu} - \tilde{\mu}_0(\tilde{T}) \tag{6}$$

Here $\tilde{P}_0(\tilde{T})$ and $\tilde{\mu}_0(\tilde{T})$ are analytic functions of $\Delta\tilde{T}$, while $\Delta\tilde{P}$ contains the singular, i.e., nonanalytic, contributions to the potential $\tilde{P}$. The equations for these functions are fully specified in Appendix A. The analytic functions are represented by truncated power series in terms of $\Delta\tilde{T}$ while the singular part $\Delta\tilde{P}$ is related to $\Delta\tilde{\mu}$ and $\Delta\tilde{T}$ with the aid of two auxiliary (parametric) variables r and θ. The computer program that generates values of the thermodynamic functions from our fundamental equation has been published elsewhere (*10*).

The fundamental equation contains the following constants: three critical parameters, P_c, T_c and ρ_c; three critical exponents, β, δ, and Δ_1; five parameters, a, k_0, k_1, c, and b^2, in the singular contribution $\Delta\tilde{P}$; four "background" parameters, $\tilde{P}_1$, $\tilde{P}_2$, $\tilde{P}_3$, and $\tilde{P}_{11}$, that specify the analytic contributions to $\tilde{P}$; and four "background" parameters, $\tilde{\mu}_c$, $\tilde{\mu}_1$, $\tilde{\mu}_2$, and $\tilde{\mu}_3$, that specify the analytic contribution to the thermal properties as a function of temperature. The three critical exponents are universal, i.e., the same for all fluids, and their "best" theoretical values are imposed on the evaluation of the other constants.

The values that we have assigned to the parameters in the fundamental equation for isobutane are listed in Appendix B. The way in which the parameters were determined is the topic of the following section. The equation is valid in the range of temperatures and densities given in eq 2.

Data Sources

The *PVT* data of Beattie et al. consist of 13 isotherms (*12*) containing 174 points in the range

$$407.764 \leq T \leq 408.314 \text{ K} \qquad 180.5 \leq \rho \leq 270.3 \text{ kg/m}^3$$

and data on a number of isotherms at higher temperatures (*13*). Of these, the 423.170 K isotherm contains six points in the density range 145.2–290.4 kg/m^3. The next higher isotherm, at 448.182 K, is outside the range of validity of our equation.

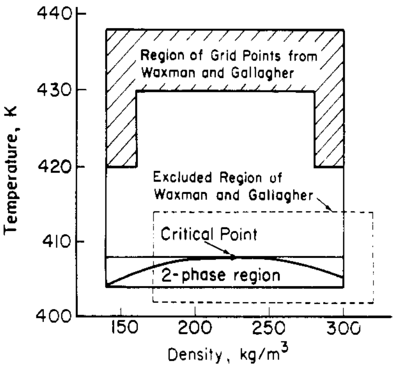

Figure 1. Range of validity of the present formulation is given by the heavy-drawn rectangle in the temperature–density plane. The dotted rectangle indicates the range excluded by Waxman and Gallagher. The hatched region is that in which data points were generated from the Waxman–Gallagher formulation in order to define our surface.

The following estimates were made of the experimental errors of the data of Beattie et al.:

$$\begin{gathered}\sigma_P = 10^{-4} \text{ MPa} \qquad \sigma_T = 0.005 \text{ K} \\ \sigma_\rho = 0.058 \text{ kg/m}^3 \text{ (0.001 mol/dm}^3) \end{gathered} \tag{7}$$

The mass of the sample was determined by weight, but the data were reported in molar units. Beattie et al. used M = 58.077 g/mol for isobutane and, in order to conserve consistency, we used this same value of M to reconvert their density data to units of kg/m^3.

For reasons given in the Introduction, we supplemented the experimental data with calculated points generated from the surface of Waxman and Gallagher (*6*). We generated 215 *PVT* data points on a grid in a region in the ρ–T space bounded, on the sides, by

$$420 \leq T \leq 438 \text{ K} \qquad 140 \leq \rho \leq 160 \text{ kg/m}^3$$

$$420 \leq T \leq 438 \text{ K} \qquad 280 \leq \rho \leq 300 \text{ kg/m}^3$$

and at the top by

$$430 \leq T \leq 438 \text{ K} \qquad 140 \leq \rho \leq 300 \text{ kg/m}^3$$

This range is indicated in Figure 1. The grid points were spaced by 2 K and 5 kg/m^3. The range around the critical point excluded by Waxman and Gallagher, eq 1, is also indicated in Figure 1.

In the fitting procedure, we have assigned the same uncertainties to the generated points as to the experimental *PVT* data. Beattie's temperatures were reported on the International Practical Temperature Scale (IPTS) of 1948. We have converted the experimental temperatures to IPTS of 1968 for the present analysis. The surface of Waxman and Gallagher was assumed to be on IPTS-68. All temperatures reported in what follows will be on IPTS-68 unless a statement to the contrary is made.

Critical-Point Parameters

Beattie et al. obtained the critical parameters of isobutane from their *PVT* data in a range of 0.6 K around T_c by a graphical construction of the coexistence dome (*12*). They obtained

$$\begin{gathered}T_c = 408.14_4 \text{ K} \qquad \rho_c = 221 \text{ kg/m}^3 \\ P_c = 3.648 \text{ MPa}\end{gathered} \tag{8}$$

It is our contention that this dome was not drawn sufficiently flat. A preliminary analysis of Beattie's data by a simple scaled equation yielded (*3*)

$$T_c = 407.865 \text{ K} \qquad \rho_c = 226.85 \text{ kg/m}^3 \qquad P_c = 3.6306 \text{ MPa} \tag{9}$$

Since scaled analyses of *PVT* data do not determine the critical temperature very precisely, one of us (J.M.H.L.S.) determined the critical temperature of 99.98% pure isobutane by observation of the meniscus disappearance, and the critical density by weight (Appendix E). The results are

$$T_c = 407.84 \pm 0.02 \text{ K} \qquad \rho_c = 225.5 \pm 2 \text{ kg/m}^3 \tag{10}$$

These values are clearly consistent with those obtained by the simple scaled analysis of Beattie's data. We have therefore, in our present analysis, imposed the observed value of T_c = 407.84 K.

If the experimental value of ρ_c, eq 10, is imposed on the fit to the present scaled equation, the reduced χ^2 equals 1.72, compared with a minimum value of 1.26 reached for ρ_c = 226.42 kg/m^3. We felt that the increase in χ^2 could be tolerated and therefore we have imposed the critical parameter values

$$T_c = 407.84 \text{ K} \qquad \rho_c = 225.5 \text{ kg/m}^3 \tag{11}$$

The critical pressure was treated as an adjustable parameter in the fit to the *PVT* data.

Equation of State Parameters

The values that we have accepted for the universal parameters β, δ, Δ_1, and b^2 (Appendix B) reflect the current theoretical knowledge (*9*) and are the same as the values that we used to represent the thermodynamic properties of light and heavy water (*10*, *11*).

The parameters a, k_0, k_1, c in the scaled contribution, and the pressure background parameters $\tilde{P}_1$, $\tilde{P}_2$, $\tilde{P}_3$, $\tilde{P}_{11}$, are system dependent. These parameters, together with the critical pressure P_c, are determined by fitting the equation of state to the *PVT* data, with the exception of $\tilde{P}_{11}$, which is determined from the slope of the diameter of the coexistence curve; this slope was deduced from the equation of Waxman et al. to be equal to −0.4971 kg/m^3, or −0.9011 in reduced units. In our analysis we found that the coefficient $\tilde{P}_3$ was not statistically significant and did not improve the accuracy of the representation; it was therefore set equal to zero.

The constant $\tilde{P}_1$ is related to the slope of the vapor pressure curve at the critical point. Our first approach was to estimate this slope by fitting Waxman's new vapor pressure data (*6*) in the range of 298.15–398.15 K with a scaled equation, while imposing our choices of P_c and T_c. The equation and the results of the fit are summarized in Appendix C. From this fit, we obtained $\tilde{P}_1$ = 5.8038. We realize, however, that the use of a scaled equation in such a large range is not justified. If $\tilde{P}_1$ is left a free parameter in the fit to Beattie's data, we obtain $\tilde{P}_1$ = 5.8858 ± 0.0015, a significantly higher value. The low value from the vapor pressure analysis cannot be reconciled with the *PVT* data. It is the high value from the *PVT* data that we have adopted for $\tilde{P}_1$.

The values of the parameters of the equation of state, obtained by fitting the PVT data of Beattie et al. plus points generated from the surface of Waxman et al. to our equation, are listed in Appendix B. The reduced χ^2 of the fit is 1.72.

In Figures 2 and 3 we show the pressure deviations of the experimental data of Beattie et al. from our surface. In Figure 3 we also show the deviations of the surface of Waxman et al. from our surface along selected isotherms as indicated by the dashed curves. Most of the Beattie data are fitted to better than 0.002 MPa and the departures of the Waxman surface from our own for temperatures 423 K and higher are also within the 0.002 MPa range.

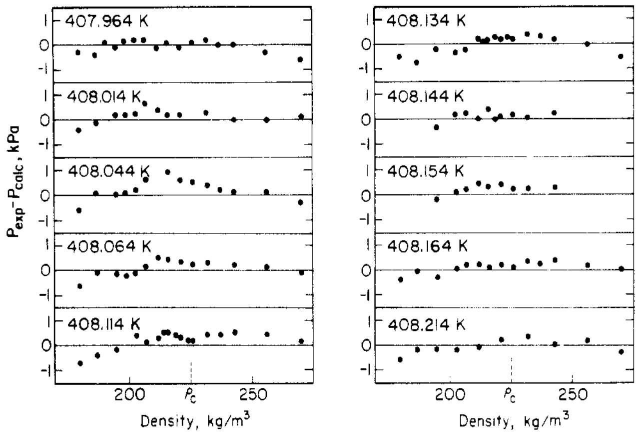

Figure 2. Departures of the isothermal *PVT* data of Beattie et al. (*12*) from our surface (1 kPa = 0.001 MPa = 0.01 bar).

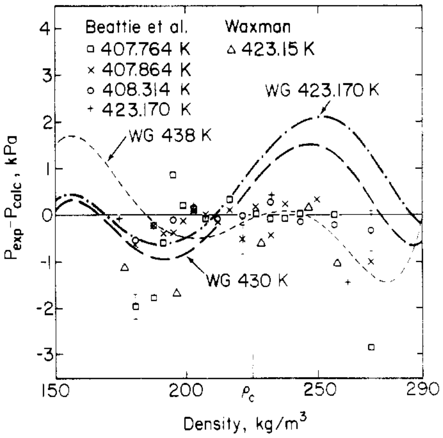

Figure 3. Departures of the *PVT* data of Beattie et al. (*12*, *13*) and of Waxman (*6*) from our surface along selected isotherms. The curves denote the departures of the Waxman–Gallagher formulation (*6*) from our surface. All depatures are well within the 0.002-MPa range (1 kPa = 0.001 MPa = 0.01 bar).

Coexistence Curve

The location of the phase boundary turned out to be the most frustrating part of the correlation. Reliable experimental data for the saturation properties are not available for the vapor above 368 K and for the liquid above 396 K. The coexistence curve that we predict is based on Beattie's *PVT* data which extend over a range of no more than 0.1 K below the critical point. Our coexistence curve ceases to be valid below 405 K. The coexistence curve prediction of Waxman and Gallagher, however, is not valid for temperatures exceeding 401.8 K, eq 1. We have compared with the coexistence curve from the correlation of Goodwin and Haynes (*7*) which equation incorporates some of the critical anomalies and has its critical point at the physical critical temperature. The comparison is shown in Table I. It is seen that the liquid densities agree on the level of 0.2%, which is excellent. The vapor densities of our equation are up to 1.8% lower than those of Goodwin and Haynes. In the absence of data above 368 K, this is probably not a bad agreement. Even though a "blend" with the Waxman surface has been our goal, we have not tried to readjust our surface in order to match up with Waxman's coexistence curve: doing this would have brought our coexistence curve further from the dome predicted by Goodwin and Haynes and would have put undue strain on our surface in other regions.

We note that classical equations lead to a coexistence dome which is not sufficiently flat (*14*). As a consequence such equations tend to imply a critical temperature which is too high (*15*). Indeed, when the analytic equation of Waxman and

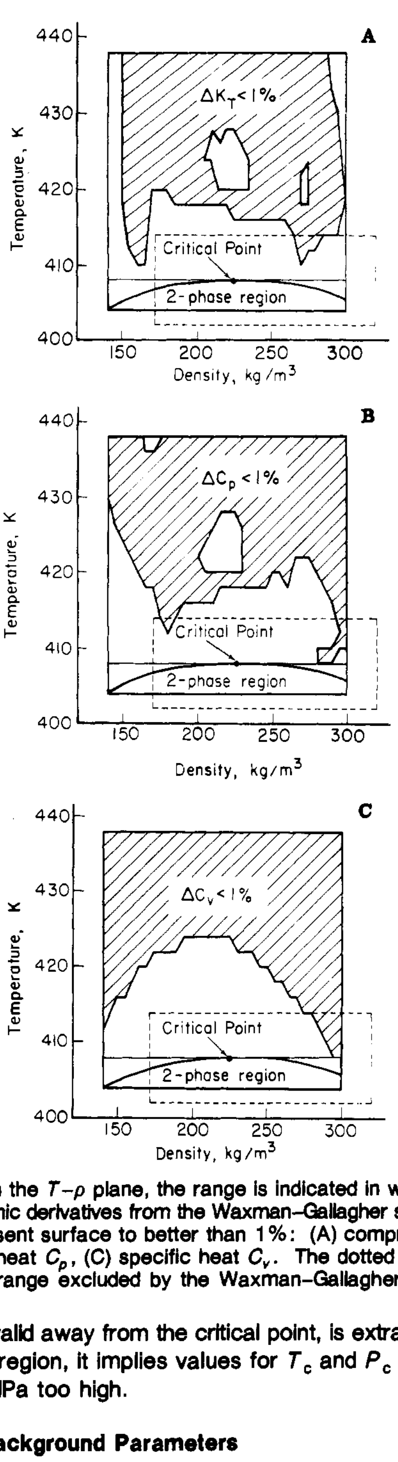

Figure 4. In the T–ρ plane, the range is indicated in which specific thermodynamic derivatives from the Waxman–Gallagher surface agree with the present surface to better than 1%: (A) compressibility K_T, (B) specific heat C_p, (C) specific heat C_v. The dotted rectangle indicates the range excluded by the Waxman–Gallagher formulation.

Gallagher, valid away from the critical point, is extrapolated into the critical region, it implies values for T_c and P_c about 1.8 K and 0.11 MPa too high.

Thermal Background Parameters

In our analyses of the thermodynamic properties of H_2O and D_2O, we used experimental data on the thermal properties such as specific heats or speed of sound to determine the thermal background parameters $\tilde{\mu}_2$ and $\tilde{\mu}_3$. Since experimental data on the thermal properties of isobutane in the critical region are not available, we used the thermodynamic surface of Waxman et al. to determine the values of the parameters $\tilde{\mu}_2$ and $\tilde{\mu}_3$.

We therefore generated isochoric specific heat, C_v, data from the equation of Waxman et al. in the range shown in Figure 1. After subtracting the scaled contributions to C_v from these generated data, we have fitted the remainder to a linear expression to determine the parameters $\tilde{\mu}_2$ and $\tilde{\mu}_3$.

First, in order to determine whether the inclusion of the background parameter $\tilde{\mu}_3$ significantly improves our surface, we set $\tilde{\mu}_3 = 0$ and fitted the C_v remainder to $\tilde{\mu}_2$. We find $\tilde{\mu}_2 = -37.705 \pm 0.023$. With this value for $\tilde{\mu}_2$, the differences in C_v calculated from our equation and that of Waxman et al. become as much as 8% in the range where both equations claim validity (Figure 1).

Table I. Comparison with the Coexistence Dome of Goodwin and Haynes

	saturated liquid densities, kg/m³			
temp, K	Goodwin	scaled	diff	diff, %
404.0	315.18	314.60	0.58	0.18
404.5	310.75	310.10	0.65	0.21
405.0	305.88	305.19	0.69	0.22
405.5	300.44	299.77	0.67	0.22
406.0	294.22	293.61	0.61	0.21
406.5	286.81	286.36	0.45	0.16
407.0	277.36	277.19	0.17	0.06
407.5	263.11	263.43	-0.32	-0.12
407.8	243.92	244.09	-0.17	-0.07

	saturated vapor densities, kg/m³			
temp, K	Goodwin	scaled	diff	diff, %
404.0	143.24	140.64	2.60	1.85
404.5	147.10	144.63	2.47	1.71
405.0	151.35	149.01	2.34	1.57
405.5	156.11	153.92	2.19	1.43
406.0	161.56	159.54	2.02	1.27
406.5	168.06	166.25	1.81	1.09
407.0	176.34	174.86	1.48	0.85
407.5	188.82	188.04	0.78	0.42
407.8	205.84	206.98	-1.14	-0.55

Table II

Critical Parameters

$T_c = 407.84$ K^a $\quad$ $P_c = 3.6290$ MPa^b

$\rho_c = 225.5$ kg/m^3 ^{a,b}

Critical Exponents

$\beta = 0.325^c$ $\quad$ $\Delta_1 = 0.50^c$

$\delta = 4.82^c$

Parameters in Scaling Functions

$a = 22.0163^b$ $\quad$ $c = -0.0096833^b$

$k_0 = 1.19385^b$ $\quad$ $b^2 = 1.3757^d$

$k_1 = 0.50552^b$

Pressure Background Parameters

$\tilde{P}_1 = 5.8858^b$ $\quad$ $\tilde{P}_3 = 0^b$

$\tilde{P}_2 = -22.0805^b$ $\quad$ $\tilde{P}_{11} = -0.068209^e$

Thermal Background Parameters

$\tilde{\mu}_c = -4.9535^f$ $\quad$ $\tilde{\mu}_2 = -32.2295^g$

$\tilde{\mu}_1 = -21.6912^f$ $\quad$ $\tilde{\mu}_3 = -33.5271^g$

[a] From direct determination. [b] From fit to PVT data. [c] Fixed from theory. [d] Same as for H_2O and D_2O. [e] From the slope of the coexistence curve diameter. [f] From identification of our surface with that of Waxman et al. at $T = 438$ K and $\rho = 205$ kg/m^3. [g] From matching our C_v with that of Waxman et al. in the range shown in Figure 1.

Next, with both $\tilde{\mu}_2$ and $\tilde{\mu}_3$ adjustable, we found

$$\tilde{\mu}_2 = -32.230 \pm 0.111$$

$$\tilde{\mu}_3 = -33.527 \pm 0.665 \qquad (12)$$

With these parameter values the differences in C_v are less than 1% throughout the above range. We therefore conclude that the presence of the parameter $\tilde{\mu}_3$ in the thermal background improves our surface significantly, and we adopt the values for the parameters $\tilde{\mu}_2$ and $\tilde{\mu}_3$ as specified in eq 12. In Figure 4 we show the regions where compressibility K_T and specific heats C_v and C_p of our equation agree with those of Waxman et al. to better than 1%.

In order to complete our equation we need to adopt values for $\tilde{\mu}_c$ and $\tilde{\mu}_1$ which are related to the zero points of entropy and energy. We determine these zero-point constants by

Table III

	temp, K	P_{exptl}, MPa	P_{calcd}, MPa	$P_{\text{exptl}} - P_{\text{calcd}}$, MPa
1	298.15	0.3500	0.3501	-0.0001
2	303.15	0.4043	0.4041	0.0002
3	308.15	0.4641	0.4640	0.0001
4	313.15	0.5304	0.5304	0.0000
5	318.15	0.6032	0.6036	-0.0004
6	323.15	0.6836	0.6840	-0.0004
7	328.15	0.7725	0.7720	0.0005
8	333.15	0.8683	0.8682	0.0001
9	333.15	0.8676	0.8682	-0.0006
10	343.15	1.0867	1.0866	0.0001
11	353.15	1.3432	1.3429	0.0003
12	363.15	1.6408	1.6411	-0.0003
13	373.15	1.9855	1.9859	-0.0004
14	383.15	2.3819	2.3821	-0.0002
15	393.15	2.8361	2.8362	-0.0001
16	398.15	3.0879	3.0875	0.0004

identifying the energy and entropy of our surface at $T = 438$ K and $\rho = 205$ kg/m^3 with the energy and entropy of the global equation of Waxman and co-workers. At this point the difference in pressures calculated from our equation and from that of Waxman et al. is 0.009%, the difference in specific heat at constant volume is 0.07%, the difference in specific heat at constant pressure is 0.1%, and the difference in compressibility is 0.07%. The condition that the values of the energy and entropy coincide with those calculated from the global surface of Waxman et al. at this point yields

$$\tilde{\mu}_c = -4.953$$

$$\tilde{\mu}_1 = -21.691 \tag{13}$$

The reference points of enthalpy and entropy of that correlation are the liquid at the normal boiling point as defined by the surface ($T = 261.395$ K for $P = 0.101325$ MPa). This completes the determination of the parameters. A complete listing

Table IV. Coexisting Phase Properties

temp, K	press., MPa	density, kg/m^3	latent heat, kJ/kg	internal energy, kJ/kg	enthalpy, kJ/kg	entropy, kJ/(kg K)	c_v, kJ/(kg K)	c_p, kJ/(kg K)	velocity of sound, m/s
				Liquid					
406.00	3.5186	293.61	68.50	413.9	425.9	1.2407	2.432	19.98	124.8
406.10	3.5245	292.27	67.11	414.7	426.7	1.2426	2.441	21.07	123.6
406.20	3.5304	290.87	65.67	415.4	427.5	1.2446	2.451	22.31	122.4
406.30	3.5363	289.43	64.17	416.2	428.4	1.2466	2.461	23.72	121.2
406.40	3.5423	287.92	62.62	416.9	429.2	1.2487	2.472	25.34	119.9
406.50	3.5482	286.36	61.01	417.7	430.1	1.2508	2.484	27.24	118.6
406.60	3.5542	284.72	59.32	418.6	431.1	1.2530	2.497	29.47	117.3
406.70	3.5601	283.00	57.55	419.4	432.0	1.2553	2.511	32.13	116.0
406.80	3.5661	281.18	55.69	420.3	433.0	1.2577	2.527	35.36	114.6
406.90	3.5721	279.25	53.72	421.3	434.0	1.2602	2.545	39.36	113.2
407.00	3.5781	277.19	51.61	422.2	435.1	1.2629	2.565	44.42	111.7
407.10	3.5841	274.97	49.35	423.3	436.3	1.2657	2.587	51.02	110.1
407.20	3.5901	272.56	46.90	424.4	437.6	1.2687	2.614	59.94	108.5
407.30	3.5962	269.89	44.19	425.6	438.9	1.2720	2.646	72.61	106.8
407.40	3.6022	266.90	41.16	426.9	440.4	1.2756	2.685	91.87	105.0
407.50	3.6083	263.43	37.65	428.4	442.1	1.2797	2.736	124.21	103.0
407.60	3.6144	259.22	33.42	430.2	444.2	1.2846	2.809	188.17	100.7
407.70	3.6205	253.65	27.84	432.5	446.8	1.2910	2.928	362.66	97.8
407.80	3.6266	244.09	18.33	436.3	451.2	1.3018	3.241	1726.56	92.6
407.84	3.6290	225.50	0.00	443.8	459.9	1.3231			0.0
				Vapor					
405.00	3.4602	149.01	80.56	476.1	499.3	1.4224	2.507	20.62	120.1
405.10	3.4660	149.95	79.47	475.8	498.9	1.4213	2.513	21.35	119.9
405.20	3.4718	150.90	78.37	475.5	498.5	1.4201	2.520	22.14	119.6
405.30	3.4776	151.88	77.23	475.1	498.0	1.4189	2.527	22.99	119.4
405.40	3.4834	152.88	76.08	474.8	497.6	1.4177	2.534	23.92	119.1
405.50	3.4893	153.91	74.89	474.4	497.1	1.4164	2.542	24.94	118.8
405.60	3.4951	154.97	73.68	474.0	496.6	1.4151	2.550	26.05	118.6
405.70	3.5010	156.06	72.44	473.6	496.1	1.4138	2.558	27.28	118.3
405.80	3.5068	157.18	71.16	473.2	495.6	1.4124	2.567	28.63	118.0
405.90	3.5127	158.34	69.85	472.8	495.0	1.4109	2.576	30.13	117.7
406.00	3.5186	159.54	68.50	472.4	494.4	1.4094	2.585	31.80	117.4
406.10	3.5245	160.78	67.11	471.9	493.8	1.4079	2.595	33.69	117.1
406.20	3.5304	162.06	65.67	471.4	493.2	1.4062	2.606	35.82	116.8
406.30	3.5363	163.40	64.17	470.9	492.6	1.4045	2.617	38.24	116.4
406.40	3.5423	164.79	62.62	470.4	491.9	1.4028	2.630	41.03	116.1
406.50	3.5482	166.25	61.01	469.8	491.1	1.4009	2.643	44.27	115.7
406.60	3.5542	167.78	59.32	469.2	490.4	1.3989	2.657	48.06	115.3
406.70	3.5601	169.39	57.55	468.5	489.6	1.3968	2.672	52.58	114.9
406.80	3.5661	171.10	55.69	467.9	488.7	1.3946	2.689	58.03	114.4
406.90	3.5721	172.92	53.72	467.1	487.8	1.3922	2.708	64.74	114.0
407.00	3.5781	174.86	51.61	466.3	486.8	1.3897	2.729	73.18	113.4
407.10	3.5841	176.96	49.35	465.4	485.7	1.3869	2.753	84.09	112.8
407.20	3.5901	179.26	46.90	464.4	484.5	1.3839	2.780	98.72	112.1
407.30	3.5962	181.81	44.19	463.3	483.1	1.3805	2.813	119.26	111.3
407.40	3.6022	184.69	41.16	462.1	481.6	1.3766	2.853	150.03	110.4
407.50	3.6083	188.04	37.65	460.6	479.8	1.3721	2.905	200.80	109.2
407.60	3.6144	192.12	33.42	458.8	477.6	1.3666	2.977	298.76	107.5
407.70	3.6205	197.55	27.84	456.3	474.6	1.3593	3.094	556.28	105.0
407.80	3.6266	206.98	18.33	452.0	469.5	1.3467	3.396	2416.05	99.0
407.84	3.6290	225.50	0.00	443.8	459.9	1.3231			0.0

Table V. Table of Thermodynamic Properties along Isotherms at Regular Density Increments

T DEG C	PRESSURE MPA	RHO KG/M3	INTERNAL ENERGY KJ/KG	ENTHALPY KJ/KG	ENTROPY KJ/(KG.K)	CP KJ/(KG.K)	CV	VELOCITY OF SOUND M/S	PHASE REGION
405.0	3.4602	150.0	475.2	498.3	1.4198		5.217		2
405.0	3.4602	160.0	466.9	488.5	1.3957		5.048		2
405.0	3.4602	170.0	459.5	479.9	1.3744		4.900		2
405.0	3.4602	180.0	453.0	472.2	1.3555		4.768		2
405.0	3.4602	190.0	447.1	465.4	1.3385		4.650		2
405.0	3.4602	200.0	441.9	459.2	1.3233		4.543		2
405.0	3.4602	210.0	437.1	453.6	1.3095		4.447		2
405.0	3.4602	220.0	432.8	448.5	1.2970		4.359		2
405.0	3.4602	230.0	428.8	443.9	1.2855		4.280		2
405.0	3.4602	240.0	425.2	439.6	1.2750		4.206		2
405.0	3.4602	250.0	421.9	435.7	1.2654		4.139		2
405.0	3.4602	260.0	418.8	432.1	1.2565		4.077		2
405.0	3.4602	270.0	416.0	428.8	1.2482		4.019		2
405.0	3.4602	280.0	413.3	425.7	1.2406		3.966		2
405.0	3.4602	290.0	410.8	422.8	1.2334		3.916		2
406.0	3.5037	150.0	478.0	501.4	1.4267	17.75	2.479	120.9	1
406.0	3.5186	160.0	472.0	494.0	1.4084		5.226		2
406.0	3.5186	170.0	464.5	485.2	1.3867		5.067		2
406.0	3.5186	180.0	457.8	477.4	1.3674		4.926		2
406.0	3.5186	190.0	451.9	470.4	1.3502		4.800		2
406.0	3.5186	200.0	446.5	464.1	1.3347		4.687		2
406.0	3.5186	210.0	441.6	458.4	1.3206		4.584		2
406.0	3.5186	220.0	437.2	453.2	1.3079		4.491		2
406.0	3.5186	230.0	433.2	448.5	1.2962		4.405		2
406.0	3.5186	240.0	429.5	444.1	1.2855		4.327		2
406.0	3.5186	250.0	426.1	440.1	1.2757		4.255		2
406.0	3.5186	260.0	422.9	436.5	1.2666		4.189		2
406.0	3.5186	270.0	420.0	433.1	1.2583		4.128		2
406.0	3.5186	280.0	417.3	429.9	1.2505		4.071		2
406.0	3.5186	290.0	414.8	426.9	1.2432		4.017		2
407.0	3.5450	150.0	480.5	504.1	1.4328	15.13	2.451	122.0	1
407.0	3.5642	160.0	474.7	496.9	1.4149	24.22	2.532	118.5	1
407.0	3.5751	170.0	469.0	490.0	1.3978	46.79	2.647	115.2	1
407.0	3.5781	180.0	462.9	482.8	1.3799		5.253		2
407.0	3.5781	190.0	456.8	475.6	1.3623		5.110		2
407.0	3.5781	200.0	451.3	469.2	1.3465		4.981		2
407.0	3.5781	210.0	446.3	463.4	1.3322		4.865		2
407.0	3.5781	220.0	441.8	458.1	1.3192		4.759		2
407.0	3.5781	230.0	437.7	453.2	1.3073		4.663		2
407.0	3.5781	240.0	433.9	448.8	1.2964		4.574		2
407.0	3.5781	250.0	430.4	444.7	1.2864		4.493		2
407.0	3.5781	260.0	427.2	441.0	1.2772		4.417		2
407.0	3.5781	270.0	424.2	437.5	1.2686		4.348		2
407.0	3.5805	280.0	421.2	434.0	1.2601	34.85	2.525	114.9	1
407.0	3.5952	290.0	417.7	430.1	1.2502	18.70	2.425	126.4	1
408.0	3.5859	150.0	482.9	506.8	1.4388	13.31	2.430	123.1	1
408.0	3.6087	160.0	477.2	499.7	1.4211	19.57	2.495	119.8	1
408.0	3.6232	170.0	471.6	492.9	1.4042	31.60	2.572	116.7	1
408.0	3.6316	180.0	466.2	486.4	1.3880	57.33	2.667	113.7	1
408.0	3.6359	190.0	461.0	480.1	1.3726	120.13	2.788	110.4	1
408.0	3.6377	200.0	456.0	474.2	1.3580	295.03	2.937	106.5	1
408.0	3.6385	210.0	451.2	468.5	1.3442	783.74	3.101	102.2	1
408.0	3.6387	220.0	446.7	463.3	1.3312	1596.97	3.208	98.4	1
408.0	3.6389	230.0	442.5	458.3	1.3191	1526.54	3.179	96.7	1
408.0	3.6392	240.0	438.5	453.7	1.3078	678.23	3.023	97.7	1
408.0	3.6400	250.0	434.7	449.3	1.2970	232.66	2.832	101.1	1
408.0	3.6421	260.0	431.0	445.0	1.2865	89.54	2.673	106.2	1
408.0	3.6474	270.0	427.4	440.9	1.2763	42.18	2.553	112.9	1
408.0	3.6586	280.0	423.7	436.8	1.2662	23.74	2.465	121.3	1
408.0	3.6794	290.0	420.1	432.8	1.2561	15.34	2.398	131.4	1
409.0	3.6265	150.0	485.3	509.5	1.4447	11.96	2.414	124.2	1
409.0	3.6528	160.0	479.7	502.5	1.4271	16.62	2.468	121.0	1
409.0	3.6707	170.0	474.2	495.8	1.4104	24.39	2.527	118.0	1
409.0	3.6823	180.0	468.8	489.3	1.3944	37.62	2.591	115.4	1
409.0	3.6896	190.0	463.7	483.1	1.3793	59.59	2.656	112.8	1
409.0	3.6941	200.0	458.8	477.3	1.3649	92.53	2.714	110.4	1
409.0	3.6971	210.0	454.1	471.7	1.3512	130.94	2.754	108.3	1
409.0	3.6993	220.0	449.6	466.4	1.3384	155.72	2.767	106.7	1
409.0	3.7013	230.0	445.4	461.5	1.3262	147.59	2.748	106.1	1
409.0	3.7037	240.0	441.3	456.8	1.3146	112.40	2.702	106.7	1
409.0	3.7071	250.0	437.4	452.3	1.3036	73.61	2.636	108.8	1
409.0	3.7126	260.0	433.6	447.9	1.2929	45.37	2.563	112.6	1
409.0	3.7221	270.0	429.9	443.7	1.2825	28.35	2.494	118.4	1
409.0	3.7383	280.0	426.2	439.5	1.2722	18.73	2.432	126.0	1
409.0	3.7648	290.0	422.5	435.4	1.2620	13.25	2.381	135.6	1
410.0	3.6668	150.0	487.7	512.2	1.4506	10.92	2.402	125.3	1
410.0	3.6965	160.0	482.1	505.2	1.4331	14.55	2.448	122.1	1
410.0	3.7177	170.0	476.7	498.5	1.4165	20.08	2.496	119.3	1
410.0	3.7325	180.0	471.4	492.1	1.4007	28.38	2.544	116.8	1
410.0	3.7428	190.0	466.3	486.0	1.3857	40.07	2.589	114.6	1
410.0	3.7500	200.0	461.5	480.2	1.3714	54.44	2.625	112.7	1
410.0	3.7554	210.0	456.8	474.7	1.3578	68.09	2.647	111.2	1
410.0	3.7598	220.0	452.3	469.4	1.3450	75.21	2.651	110.3	1
410.0	3.7642	230.0	448.1	464.4	1.3328	71.70	2.637	110.1	1
410.0	3.7690	240.0	444.0	459.7	1.3211	59.42	2.605	111.0	1
410.0	3.7753	250.0	440.0	455.1	1.3099	44.35	2.561	113.2	1
410.0	3.7843	260.0	436.2	450.7	1.2991	31.32	2.510	117.0	1
410.0	3.7980	270.0	432.4	446.4	1.2885	21.94	2.459	122.6	1
410.0	3.8191	280.0	428.6	442.2	1.2781	15.76	2.411	130.0	1
410.0	3.8511	290.0	424.8	438.1	1.2678	11.80	2.369	139.3	1
415.0	3.8652	150.0	499.6	525.4	1.4794	7.93	2.365	130.7	1
415.0	3.9112	160.0	494.2	518.6	1.4624	9.45	2.393	127.9	1
415.0	3.9486	170.0	488.9	512.1	1.4462	11.32	2.419	125.5	1
415.0	3.9791	180.0	483.8	505.9	1.4308	13.49	2.441	123.5	1
415.0	4.0044	190.0	478.9	499.9	1.4161	15.80	2.459	122.1	1
415.0	4.0260	200.0	474.1	494.2	1.4020	17.91	2.471	121.2	1
415.0	4.0453	210.0	469.5	488.8	1.3886	19.42	2.476	120.8	1
415.0	4.0636	220.0	465.0	483.5	1.3758	19.95	2.475	121.1	1
415.0	4.0821	230.0	460.7	478.5	1.3634	19.37	2.467	122.2	1
415.0	4.1021	240.0	456.5	473.6	1.3515	17.84	2.453	124.3	1
415.0	4.1252	250.0	452.4	468.9	1.3400	15.74	2.435	127.4	1
415.0	4.1531	260.0	448.4	464.4	1.3288	13.49	2.413	131.9	1
415.0	4.1883	270.0	444.5	460.0	1.3178	11.40	2.390	137.8	1
415.0	4.2338	280.0	440.5	455.6	1.3070	9.63	2.366	145.2	1
415.0	4.2932	290.0	436.6	451.4	1.2963	8.20	2.343	154.2	1
420.0	4.0595	150.0	511.4	538.5	1.5076	6.49	2.350	136.1	1
420.0	4.1217	160.0	506.1	531.9	1.4909	7.35	2.371	133.5	1
420.0	4.1751	170.0	500.9	525.5	1.4750	8.31	2.389	131.4	1
420.0	4.2215	180.0	495.9	519.4	1.4598	9.34	2.404	129.8	1
420.0	4.2625	190.0	491.0	513.5	1.4452	10.33	2.415	128.8	1
420.0	4.2997	200.0	486.3	507.8	1.4313	11.16	2.423	128.4	1
420.0	4.3346	210.0	481.7	502.4	1.4179	11.70	2.426	128.7	1
420.0	4.3688	220.0	477.3	497.1	1.4051	11.87	2.425	129.7	1
420.0	4.4038	230.0	472.9	492.1	1.3926	11.63	2.419	131.5	1
420.0	4.4413	240.0	468.7	487.2	1.3806	11.04	2.411	134.2	1
420.0	4.4832	250.0	464.5	482.4	1.3689	10.21	2.399	138.0	1
420.0	4.5317	260.0	460.4	477.8	1.3575	9.27	2.386	143.1	1
420.0	4.5895	270.0	456.3	473.3	1.3463	8.32	2.371	149.4	1
420.0	4.6600	280.0	452.3	469.0	1.3353	7.44	2.355	157.0	1
420.0	4.7470	290.0	448.3	464.7	1.3243	6.68	2.340	166.1	1
425.0	4.2509	150.0	523.1	551.5	1.5354	5.64	2.345	141.3	1
425.0	4.3291	160.0	517.9	545.0	1.5189	6.20	2.362	139.0	1
425.0	4.3987	170.0	512.8	538.7	1.5032	6.80	2.376	137.2	1
425.0	4.4612	180.0	507.9	532.7	1.4881	7.40	2.388	135.9	1
425.0	4.5185	190.0	503.1	526.8	1.4737	7.96	2.396	135.3	1
425.0	4.5720	200.0	498.4	521.2	1.4598	8.41	2.402	135.3	1
425.0	4.6236	210.0	493.8	515.8	1.4465	8.69	2.405	136.0	1
425.0	4.6749	220.0	489.3	510.6	1.4336	8.78	2.404	137.5	1
425.0	4.7277	230.0	485.0	505.5	1.4211	8.65	2.401	139.8	1
425.0	4.7840	240.0	480.7	500.6	1.4090	8.34	2.395	143.1	1
425.0	4.8460	250.0	476.5	495.8	1.3972	7.90	2.387	147.4	1
425.0	4.9162	260.0	472.3	491.2	1.3857	7.38	2.377	152.8	1
425.0	4.9976	270.0	468.2	486.7	1.3743	6.83	2.366	159.5	1
425.0	5.0937	280.0	464.1	482.3	1.3631	6.30	2.355	167.4	1
425.0	5.2086	290.0	460.0	478.0	1.3520	5.81	2.344	176.6	1
430.0	4.4400	150.0	534.9	564.5	1.5628	5.07	2.344	146.3	1
430.0	4.5342	160.0	529.7	558.1	1.5465	5.47	2.358	144.3	1
430.0	4.6200	170.0	524.7	551.9	1.5309	5.89	2.370	142.8	1
430.0	4.6990	180.0	519.8	545.9	1.5160	6.29	2.380	141.9	1
430.0	4.7729	190.0	515.0	540.1	1.5017	6.65	2.388	141.6	1
430.0	4.8434	200.0	510.4	534.6	1.4879	6.94	2.393	141.9	1
430.0	4.9124	210.0	505.8	529.2	1.4745	7.12	2.395	143.0	1
430.0	4.9816	220.0	501.3	524.0	1.4617	7.17	2.395	144.8	1
430.0	5.0531	230.0	496.9	518.9	1.4492	7.10	2.393	147.6	1
430.0	5.1291	240.0	492.6	514.0	1.4370	6.91	2.389	151.3	1
430.0	5.2121	250.0	488.4	509.2	1.4251	6.64	2.383	156.0	1
430.0	5.3048	260.0	484.2	504.6	1.4135	6.31	2.376	161.8	1
430.0	5.4104	270.0	480.0	500.1	1.4020	5.95	2.368	168.7	1
430.0	5.5327	280.0	475.9	495.6	1.3907	5.60	2.360	176.9	1
430.0	5.6758	290.0	471.7	491.3	1.3795	5.26	2.351	186.2	1
435.0	4.6270	150.0	546.6	577.4	1.5899	4.68	2.344	151.3	1
435.0	4.7373	160.0	541.5	571.1	1.5738	4.98	2.357	149.6	1
435.0	4.8395	170.0	536.5	565.0	1.5583	5.28	2.368	148.4	1
435.0	4.9352	180.0	531.7	559.1	1.5435	5.58	2.377	147.7	1
435.0	5.0261	190.0	527.0	553.4	1.5292	5.83	2.384	147.7	1
435.0	5.1140	200.0	522.3	547.9	1.5155	6.04	2.389	148.3	1
435.0	5.2008	210.0	517.8	542.5	1.5022	6.16	2.391	149.7	1
435.0	5.2886	220.0	513.3	537.3	1.4893	6.20	2.391	151.9	1
435.0	5.3796	230.0	508.9	532.3	1.4768	6.16	2.390	155.0	1
435.0	5.4760	240.0	504.6	527.4	1.4646	6.03	2.387	159.0	1
435.0	5.5806	250.0	500.3	522.6	1.4527	5.85	2.383	164.0	1
435.0	5.6964	260.0	496.1	518.0	1.4409	5.62	2.378	170.1	1
435.0	5.8267	270.0	491.9	513.4	1.4294	5.37	2.372	177.4	1
435.0	5.9755	280.0	487.7	509.0	1.4180	5.12	2.365	185.7	1
435.0	6.1471	290.0	483.5	504.7	1.4067	4.87	2.359	195.2	1
438.0	4.7383	150.0	553.6	585.2	1.6060	4.49	2.345	154.3	1
438.0	4.8582	160.0	548.6	578.9	1.5900	4.75	2.357	152.7	1
438.0	4.9703	170.0	543.7	572.9	1.5746	5.01	2.368	151.6	1
438.0	5.0761	180.0	538.8	567.0	1.5598	5.26	2.376	151.1	1
438.0	5.1774	190.0	534.1	561.4	1.5456	5.47	2.383	151.3	1
438.0	5.2759	200.0	529.5	555.9	1.5319	5.64	2.387	152.1	1
438.0	5.3738	210.0	524.9	550.5	1.5186	5.75	2.390	153.6	1
438.0	5.4729	220.0	520.5	545.3	1.5058	5.79	2.391	156.0	1
438.0	5.5758	230.0	516.1	540.3	1.4932	5.75	2.390	159.3	1
438.0	5.6847	240.0	511.7	535.4	1.4810	5.65	2.387	163.5	1
438.0	5.8026	250.0	507.4	530.7	1.4690	5.50	2.384	168.7	1
438.0	5.9324	260.0	503.2	526.0	1.4573	5.32	2.380	175.0	1
438.0	6.0778	270.0	499.0	521.5	1.4457	5.11	2.375	182.3	1
438.0	6.2428	280.0	494.8	517.1	1.4343	4.90	2.369	190.7	1
438.0	6.4316	290.0	490.6	512.8	1.4229	4.69	2.363	200.3	1

is given in Appendix B. In Appendix D we give tables of thermodynamic properties of isobutane as derived from our surface.

Discussion

The present formulation supplements that of Waxman and Gallagher (*6*) in most of the region around the critical point excluded by these authors. In the part of the supercritical range where both formulations claim validity, the agreement is excellent; at given density and temperature pressures agree within 0.002 MPa, enthalpies within a few tenths, and entropies within a few thousandths of an SI unit. Discrepancies exist near the phase boundary; neither equation claims validity in the range 401.8–405 K. If both equations are extrapolated to 404 K, the coexisting densities differ by percents, and the enthalpies by a few SI units.

We have refrained from comparing with earlier formulations constructed prior to the availability of the new data. The only other correlation making use of the expanded data base is that of Goodwin and Haynes (*7*). As mentioned, our coexistence curve agrees with theirs about as well as might be hoped for, given the absence of experimental saturation data above 400 K. In the supercritical range, however, the pressures of the Goodwin–Haynes correlation differ from the Beattie data, and therefore from our surface and from that of Waxman, by substantial amounts ranging, at 423 K, from +0.01 MPa at 116 kg/m^3, to +0.08 MPa at 290 kg/m^3.

Acknowledgment

We have profited from discussions with Prof. J. Kestin, M. Waxman, and Dr. D. Garvin.

Appendix A

Revised and Extended Scaling Equations for the Thermodynamic Properties of Fluids.

Reduced Thermodynamic Quantities:

$$\tilde{T} = -\frac{T_c}{T} \qquad \tilde{\mu} = \frac{\mu}{T}\frac{\rho_c T_c}{P_c} \qquad \tilde{P} = \frac{P}{T}\frac{T_c}{P_c}$$

$$\tilde{\rho} = \frac{\rho}{\rho_c} \qquad \tilde{U} = \frac{U}{V}\frac{1}{P_c} \qquad \tilde{S} = \frac{S}{V}\frac{T_c}{P_c}$$

$$\tilde{A} = \frac{A}{VT}\frac{T_c}{P_c} \qquad \tilde{H} = \frac{H}{VT}\frac{T_c}{P_c} \qquad \tilde{\chi}_T = \left(\frac{\partial\tilde{\rho}}{\partial\tilde{\mu}}\right)_T$$

$$\tilde{C}_v = \frac{C_v}{V}\frac{T_c}{P_c} \qquad \tilde{C}_P = \frac{C_p}{V}\frac{T_c}{P_c} \tag{A.1}$$

(T is temperature, μ is chemical potential, P is pressure, ρ is density, U is energy, S is entropy, A is Helmholtz free energy, H is enthalpy, V is volume, C_v is heat capacity at constant V, C_p is heat capacity at constant P).

Thermodynamic Relations:

$$\begin{aligned} d\tilde{P} &= \tilde{U}\,d\tilde{T} + \tilde{\rho}\,d\tilde{\mu} \\ d\tilde{A} &= -\tilde{U}\,d\tilde{T} + \tilde{\mu}\,d\tilde{\rho} \\ d\tilde{H} &= -\tilde{T}\,d\tilde{U} + \tilde{\rho}\,d\tilde{\mu} \\ d\tilde{S} &= -\tilde{T}\,d\tilde{U} - \tilde{\mu}\,d\tilde{\rho} \end{aligned} \tag{A.2}$$

with

$$\begin{aligned} \tilde{A} &= \tilde{\rho}\tilde{\mu} - \tilde{P} \\ \tilde{H} &= \tilde{P} - \tilde{T}\tilde{U} \\ \tilde{S} &= \tilde{H} - \tilde{\rho}\tilde{\mu} = -\tilde{T}\tilde{U} - \tilde{A} \end{aligned} \tag{A.3}$$

Fundamental Equations:

$$\Delta\tilde{T} = \tilde{T} + 1 \tag{A.4a}$$

$$\Delta\tilde{\mu} = \tilde{\mu} - \tilde{\mu}_0(\tilde{T}) \tag{A.4b}$$

$$\tilde{P} = \tilde{P}_0(\tilde{T}) + \Delta\tilde{\mu} + \tilde{P}_{11}\Delta\tilde{\mu}\Delta\tilde{T} + \Delta\tilde{P} \tag{A.5}$$

with

$$\tilde{\mu}_0(\tilde{T}) = \tilde{\mu}_c + \sum_{j=1}^{3} \tilde{\mu}_j(\Delta\tilde{T})^j \tag{A.6a}$$

$$\tilde{P}_0(\tilde{T}) = 1 + \sum_{j=1}^{3} \tilde{P}_j(\Delta\tilde{T})^j \tag{A.6b}$$

Derived Thermodynamic Quantities:

$$\tilde{\rho} = 1 + \tilde{P}_{11}\Delta\tilde{T} + (\partial\Delta\tilde{P}/\partial\Delta\tilde{\mu})_{\Delta\tilde{T}} \tag{A.7}$$

$$\tilde{U} = \frac{d\tilde{P}_0}{d\tilde{T}} - \tilde{\rho}\frac{d\tilde{\mu}_0}{d\tilde{T}} + \tilde{P}_{11}\Delta\tilde{\mu} + \left(\frac{\partial\Delta\tilde{P}}{\partial\Delta\tilde{T}}\right)_{\Delta\tilde{\mu}} \tag{A.8}$$

$$\tilde{\chi}_T = (\partial^2\Delta\tilde{P}/\partial\Delta\tilde{\mu}^2)_{\Delta\tilde{T}} \tag{A.9}$$

$$\left(\frac{\partial\tilde{P}}{\partial\tilde{T}}\right)_{\tilde{\rho}} = \frac{d\tilde{P}_0}{d\tilde{T}} + \tilde{P}_{11}\left[\Delta\tilde{\mu} - \frac{\tilde{\rho}}{\tilde{\chi}_T}\right] + \left(\frac{\partial\Delta\tilde{P}}{\partial\Delta\tilde{T}}\right)_{\Delta\tilde{\mu}} - \frac{\tilde{\rho}}{\tilde{\chi}_T}\frac{\partial^2\Delta\tilde{P}}{\partial\Delta\tilde{\mu}\,\partial\Delta\tilde{T}} \tag{A.10}$$

$$\frac{\tilde{C}_v}{\tilde{T}^2} = \frac{d^2\tilde{P}_0}{d\tilde{T}^2} - \tilde{\rho}\frac{d^2\tilde{\mu}_0}{d\tilde{T}^2} - \frac{\tilde{P}_{11}{}^2}{\tilde{\chi}_T} + \left(\frac{\partial^2\Delta\tilde{P}}{\partial\Delta\tilde{T}^2}\right)_{\Delta\tilde{\mu}} - \frac{2\tilde{P}_{11}}{\tilde{\chi}_T}\frac{\partial^2\Delta\tilde{P}}{\partial\Delta\tilde{\mu}\,\partial\Delta\tilde{T}} - \frac{1}{\tilde{\chi}_T}\left(\frac{\partial^2\Delta\tilde{P}}{\partial\Delta\tilde{\mu}\,\partial\Delta\tilde{T}}\right)^2 \tag{A.11}$$

$$\tilde{C}_p = \tilde{C}_v + \frac{\tilde{\chi}_T}{\tilde{\rho}^2}\left[\tilde{P} - \tilde{T}\left(\frac{\partial\tilde{P}}{\partial\tilde{T}}\right)_{\tilde{\rho}}\right]^2 \tag{A.12}$$

Critical Exponents:

$$\begin{aligned} \alpha_0 &= \alpha & \alpha_1 &= \alpha - \Delta_1 \\ \beta_0 &= \beta & \beta_1 &= \beta + \Delta_1 \\ \gamma_0 &= \gamma & \gamma_1 &= \gamma - \Delta_1 \end{aligned} \tag{A.13}$$

with

$$2 - \alpha = \beta(\delta + 1) \qquad \gamma = \beta(\delta - 1) \tag{A.14}$$

Parametric Equations for Singular Terms:

$$\Delta\tilde{\mu} = r^{\beta\delta}a\,\theta(1 - \theta^2) \tag{A.15}$$

$$\Delta\tilde{T} = r(1 - b^2\theta^2) - c\,\Delta\tilde{\mu} \tag{A.16}$$

$$\Delta\tilde{P} = \sum_{i=0}^{1} r^{2-\alpha_i}ak_i\,p_i(\theta) \tag{A.17}$$

$$(\partial\Delta\tilde{P}/\partial\Delta\tilde{\mu})_{\Delta\tilde{T}} = \sum_{i=0}^{1} [r^{\beta_i}k_i\theta + cr^{1-\alpha_i}ak_is_i(\theta)] \tag{A.18}$$

$$(\partial\Delta\tilde{P}/\partial\Delta\tilde{T})_{\Delta\tilde{\mu}} = \sum_{i=0}^{1} r^{1-\alpha_i}ak_is_i(\theta) \tag{A.19}$$

$$(\partial^2\Delta\tilde{P}/\partial\Delta\tilde{\mu}^2)_{\Delta\tilde{T}} = \sum_{i=0}^{1}\left[r^{-\gamma_i}\frac{k_i}{a}u_i(\theta) + 2cr^{\beta_i-1}k_iv_i(\theta) + c^2r^{-\alpha_i}ak_iw_i(\theta)\right] \tag{A.20}$$

$$\frac{\partial^2\Delta\tilde{P}}{\partial\Delta\tilde{\mu}\Delta\tilde{T}} = \sum_{i=0}^{1} [r^{\beta_i-1}k_iv_i(\theta) + cr^{-\alpha_i}ak_iw_i(\theta)] \tag{A.21}$$

$$(\partial^2\Delta\tilde{P}/\partial\Delta\tilde{T}^2)_{\Delta\tilde{\mu}} = \sum_{i=0}^{1} r^{-\alpha_i}ak_iw_i(\theta) \tag{A.22}$$

Auxiliary Functions:

$$p_i(\theta) = p_{0i} + p_{2i}\theta^2 + p_{4i}\theta^4 \tag{A.23}$$

$$s_i(\theta) = s_{0i} + s_{2i}\theta^2 \qquad s_i'(\theta) = 2s_{2i}\theta \tag{A.24}$$

$$q(\theta) = 1 + \{b^2(2\beta\delta - 1) - 3\}\theta^2 - b^2(2\beta\delta - 3)\theta^4 \tag{A.25}$$

$$u_i(\theta) = [1 - b^2(1 - 2\beta_i)\theta^2]/q(\theta) \tag{A.26}$$

$$v_i(\theta) = [\beta_i(1 - 3\theta^2)\theta - \beta\delta(1 - \theta^2)\theta]/q(\theta) \tag{A.27}$$

$$w_i(\theta) = [(1 - \alpha_i)(1 - 3\theta^2)s_i(\theta) - \beta\delta(1 - \theta^2)\theta s_i'(\theta)]/q(\theta) \tag{A.28}$$

with

$$\begin{aligned} p_{0i} &= +\frac{\beta\delta - 3\beta_i - b^2\alpha_i\gamma_i}{2b^4(2 - \alpha_i)(1 - \alpha_i)\alpha_i} \\ p_{2i} &= -\frac{\beta\delta - 3\beta_i - b^2\alpha_i(2\beta\delta - 1)}{2b^2(1 - \alpha_i)\alpha_i} \\ p_{4i} &= +\frac{2\beta\delta - 3}{2\alpha_i} \end{aligned} \tag{A.29}$$

$$\begin{aligned} s_{0i} &= (2 - \alpha_i)p_{0i} \\ s_{2i} &= -\frac{\beta\delta - 3\beta_i}{2b^2\alpha_i} \end{aligned} \tag{A.30}$$

Two-Phase Properties:

variables

$$\theta = \pm 1$$

$$\Delta\tilde{\mu} = 0$$

$$\Delta\tilde{T} = r(1 - b^2) \tag{A.31}$$

vapor pressure

$$\tilde{P}_{\text{vap}} = \tilde{P}_0(\tilde{T}) + \sum_{l=0}^{1} r^{2-\alpha_l} a k_l\, p_l(1) \tag{A.32}$$

coexisting densities

$$(\tilde{\rho}_{\text{L}} + \tilde{\rho}_{\text{V}})/2 = 1 + \tilde{P}_{11}\Delta\tilde{T} + \sum_{l=0}^{1} c r^{1-\alpha_l} a k_l s_l(1)$$

$$(\tilde{\rho}_{\text{L}} - \tilde{\rho}_{\text{V}})/2 = \sum_{l=0}^{1} r^{\beta_l} k_l \tag{A.33}$$

Helmholtz free energy

$$\tilde{A} = \tilde{\rho}\tilde{\mu}_0(\tilde{T}) - \tilde{P}_0(\tilde{T}) - \sum_{l=0}^{1} r^{2-\alpha_l} a k_l\, p_l(1) \tag{A.34}$$

energy

$$\tilde{U} = \frac{\mathrm{d}\tilde{P}_0}{\mathrm{d}\tilde{T}} - \tilde{\rho}\frac{\mathrm{d}\tilde{\mu}_0(\tilde{T})}{\mathrm{d}\tilde{T}} + \frac{1}{1 - b^2}\sum_{l=0}^{1} (2 - \alpha_l) r^{1-\alpha_l} a k_l\, p_l(1) \tag{A.35}$$

entropy

$$\tilde{S} = -\tilde{\rho}\tilde{\mu}_0(\tilde{T}) + \tilde{P}_0(\tilde{T}) - \tilde{T}\left[\frac{\mathrm{d}\tilde{P}_0}{\mathrm{d}\tilde{T}} - \tilde{\rho}\frac{\mathrm{d}\tilde{\mu}_0}{\mathrm{d}\tilde{T}}\right] + \sum_{l=0}^{1} r^{2-\alpha_l} a k_l\, p_l(1) - \frac{\tilde{T}}{1 - b^2}\sum_{l=0}^{1} (2 - \alpha_l) r^{1-\alpha_l} a k_l\, p_l(1) \tag{A.36}$$

specific heat C_v

$$\frac{\tilde{C}_v}{\tilde{T}^2} = \frac{\mathrm{d}^2\tilde{P}_0}{\mathrm{d}\tilde{T}^2} - \tilde{\rho}\frac{\mathrm{d}^2\tilde{\mu}_0}{\mathrm{d}\tilde{T}^2} + \left(\frac{1}{1 - b^2}\right)^2 \sum_{l=0}^{1} (2 - \alpha_l)(1 - \alpha_l) r^{-\alpha_l} a k_l\, p_l(1) \tag{A.37}$$

Appendix B

Parameter values are listed in Table II.

Appendix C

Vapor Pressure of Isobutane. The vapor pressure data of Waxman (*5*) in the range 298–398 K were fitted to the simple scaled equation

$$P^* = 1 + A_1\Delta T^* + A^-(\Delta T^*)^{2-\alpha} + A_2(\Delta T^*)^2 + A_3(\Delta T^*)^3 \tag{C.1}$$

where $P^* = P/P_c$, $\Delta T^* = (T_c - T)/T_c$ and the critical exponent $\alpha = 0.1085$. Choosing $T_c = 407.84$ K, $P_c = 3.6290$ MPa, we obtain $A_1 = -6.8038$, $A^- = 21.5688$, $A_2 = -10.1751$, $A_3 = -7.0260$ and the deviations listed in Table III.

This fit corresponds with a value of $\tilde{P}_1$ of 5.8038. Retaining the form of the vapor pressure equation, eq C.1 and the choice of T_c, we can obtain higher values of $\tilde{P}_1$ only by raising P_c. We would have to raise P_c by as much as 0.07 MPa to obtain a value $\tilde{P}_1 = 5.88$ consistent with Beattie's *PVT* data. This choice of P_c, however, would be quite inconsistent with Beattie's and Waxman's supercritical *PVT* data.

Appendix D

Tables of Thermodynamic Properties. In Table IV we list the values of the thermodynamic properties of isobutane along the coexistence curve on the liquid and vapor sides as a function of temperature. In Table V we have tabulated the thermodynamic properties along isotherms at regular density increments.

Appendix E

Measurement of the Critical Density and Temperature of Isobutane. The critical temperature and density of isobutane were determined by observation of the disappearance of the meniscus in the center of an optical cell. The cell was formed by clamping a 316 stainless-steel ring of i.d. 25.4 mm, o.d. 35 mm, and thickness 12.7 mm between two sapphire disks of o.d. 35 mm and thickness 6 mm, with tin foil of 0.025-mm thickness serving as a gasket. A steel capillary with an o.d. of 1.6 mm was welded into the steel ring and connected to a pressure valve. The volume of the cell was calculated from its dimensions to be 6.448 cm^3 at room temperature. The cell volume was corrected for the volume of the line and valve (+0.022 cm^3) and that of a small magnetic bar (−0.123 cm^3) which was used as a stirrer. The volume of the cell at higher temperatures was calculated by using the value 16.5×10^{-6}/K for the average coefficient of linear thermal expansion of the steel ring for temperatures between room temperature and 408 K.

The cell was filled with a sample of isobutane from the same research-grade supply used by Waxman for his *PVT* measurements (*6*) and certified by the supplier to be at least 99.9% pure. The amount of isobutane was determined by weighing the cell before and after filling it and was chosen such that the density exceeded the critical density by about 8%. The weighings were done on an analytical balance with a precision to within 0.5 mg.

The cell assembly was immersed in a commercial regulated bath which was provided with windows and filled with high-viscosity silicone oil. The temperature was controlled to ±0.01 K and measured by a platinum resistance thermometer and a 7-decade Mueller bridge. The resistance thermometer had been calibrated at NBS and its indication at the water triple point was monitored during the experiments.

The bath was heated and the meniscus was observed to disappear at the top of the cell. Small amounts of isobutane were subsequently released and trapped above water inside an inverted graduated glass. An account was kept of the amounts of isobutane released (in 15 steps, from 8% above to 8% below the critical density). The critical temperature and density were taken as those corresponding to the case where the meniscus disappeared in the center of the cell. At the end of the experiments the cell was weighed again. The weight loss was found to be 230 mg—it differed from the loss calculated from the volumes released by 15 mg. Since the weight of the critical sample was 1.435 g, we estimate it to be known to better than 15 mg or 1%.

For the seven different fill densities at which the meniscus disappeared at some level inside the cell, the measured temperatures of meniscus disappearance varied from 407.83 to 407.85 K.

Thus, we conclude that $T_c = 407.84 \pm 0.02$ K and $\rho_c = 225.5 \pm 2$ kg/m^3.

Thermodynamic Properties

P	pressure
P_c	critical pressure
T	temperature
T_c	critical temperature

V	volume
V_c	critical volume
ρ	density
ρ_c	critical density
μ	chemical potential
A	Helmholtz free energy
H	enthalpy
U	energy
S	entropy
K_T	isothermal compressibility
C_p	specific heat at constant pressure
C_v	specific heat at constant volume
M	molecular weight, $M = 0.0581243$ kg/mol
R	gas constant, $R = 143.045$ J/(kg K)
σ_p	experimental error in the pressure
σ_T	experimental error in the temperature
σ_ρ	experimental error in the density

Reduced Thermodynamic Properties

$\tilde{P}$	reduced pressure, $PT_c/(P_cT)$
$\Delta\tilde{P}$	singular part of $\tilde{P}$
$\tilde{T}$	reduced temperature, $-T_c/T$
$\Delta\tilde{T}$	$\tilde{T} + 1$
$\tilde{\rho}$	reduced density, ρ/ρ_c
$\tilde{\mu}$	reduced chemical potential, $\mu\rho_cT_c/(P_cT)$
$\tilde{\mu}_0(\tilde{T})$	chemical potential on the saturation curve and its analytic continuation
$\Delta\tilde{\mu}$	$\tilde{\mu} - \tilde{\mu}_0(\tilde{T})$
$\tilde{A}$	reduced Helmholtz free energy density, $AT_c/(VTP_c)$
$\tilde{H}$	reduced enthalpy density, $HT_c/(VTP_c)$
$\tilde{U}$	reduced energy density, $U/(VP_c)$
$\tilde{S}$	reduced entropy density, $ST_c/(VP_c)$
$\tilde{\chi}_T$	reduced susceptibility, $K_TV_c^2P_cT/(V^2T_c)$
$\tilde{C}_p$	reduced specific heat density, $C_vT_c/(VP_c)$
$\tilde{C}_v$	reduced specific heat density $C_pT_c/(VP_c)$

Critical Exponents

$\alpha \equiv \alpha_0$	critical exponent for the specific heat
$\beta \equiv \beta_0$	critical exponent for the coexistence curve
$\gamma \equiv \gamma_0$	critical exponent for the compressibility
δ	critical exponent for the critical isotherm
Δ_1	gap exponent for first Wegner correction
α_1	$\alpha_0 - \Delta_1$
β_1	$\beta_0 + \Delta_1$
γ_1	$\gamma_0 - \Delta_1$

Parametric Scaled Equation

r	parametric distance variable
θ	parametric contour variable
a, k_0, k_1, c, b^2	constants in scaled equation
$\tilde{P}_0(\tilde{T})$	analytic part of the vapor pressure equation
$\tilde{P}_1$, $\tilde{P}_2$, $\tilde{P}_3$	coefficients of $\tilde{P}_0(\tilde{T})$ written as a polynomial in $\tilde{T}$
$\tilde{P}_{11}$	coefficient of the term $(\Delta\tilde{\mu})(\Delta\tilde{T})$ in the expression for $\tilde{P}$
μ_1, $\tilde{\mu}_2$, $\tilde{\mu}_3$	coefficients of $\tilde{\mu}_0(\tilde{T})$ as a polynomial in $\tilde{T}$
$p_i(\theta)$, $s_i(\theta)$, $q_i(\theta)$	polynomials in θ, $i = 0, 1$
$u_i(\theta)$, $v_i(\theta)$, $w_i(\theta)$	ratios of polynomials in θ, $i = 0, 1$
p_{0i}, p_{2i}, p_{4i}	coefficients of the polynomials $p_i(\theta)$
s_{0i}, s_{2i}	coefficients of the polynomials $s_i(\theta)$

Registry No. Isobutane, 75-28-5.

Literature Cited

(1) Kestin, J.; Khalifa, H. E. In "Sourcebook on the Production of Electricity from Geothermal Energy"; Kestin, J., Editor-in-Chief; U.S. Department of Energy: Washington, DC, 1980; Chapter 4.2.2, p 351.

(2) Khalifa, H. E.; Kestin, J. In "The Technological Importance of Accurate Thermophysical Property Information"; Sengers, J. V., Klein, M., Eds.; U.S. Government Printing Office; Washington, DC, 1980; *NBS Spec. Publ.* (*U.S.*) No. 590, p 19.

(3) Waxman, M.; Davis, H. A.; Levelt Sengers, J. M. H.; Klein, M. Internal Report No. 79-1715; National Bureau of Standards: Washington, DC, 1981; available from National Technical Information Service, Department of Commerce (U.S.), Report PB82-120528.

(4) Waxman, M.; Klein, M.; Gallagher, J.; Levelt Sengers, J. M. H. Internal Report 81-2435; National Bureau of Standards: Washington, DC, 1982; available from National Technical Information Service, Department of Commerce (U.S.), Report PB83-111005.

(5) Waxman, M.; Gallagher, J. S. In "Proceedings of the 8th Symposium on Thermophysical Properties"; Sengers, J. V., Ed.; American Society of Mechanical Engineers: New York, 1982; Vol. 1, p 88.

(6) Waxman, M.; Gallagher, J. S. *J. Chem. Eng. Data* **1983**, *28*, 224.

(7) Goodwin, R. D.; Haynes, W. M. *NBS Tech. Note* (*U.S.*) **1982** *No. 1051*. Haynes, W. M., submitted to *J. Chem. Eng. Data*.

(8) Haar, L.; Gallagher, J. S.; Kell, G. S. In "Proceedings of the 8th Symposium on Thermophysical Properties"; Sengers, J. V., Ed.; American Society of Mechanical Engineers: New York, 1982; p 298.

(9) Levelt Sengers, J. M. H.; Sengers, J. V. In "Perspectives in Statistical Physics"; Raveché, H. J., Ed.; North-Holland Publishing Co.: Amsterdam, 1981; p 239.

(10) Levelt Sengers, J. M. H.; Kamgar-Parsi, B.; Balfour, F. W.; Sengers, J. V. *J. Phys. Chem. Ref. Data*, in press.

(11) Kamgar-Parsi, B.; Levelt Sengers, J. M. H.; Sengers, J. V. *J. Phys. Chem. Ref. Data*, in press.

(12) Beattie, J. A.; Edwards, D. G.; Marple, S., Jr. *J. Chem. Phys.* **1949**, *17*, 576.

(13) Beattie, J. A.; Marple, S., Jr.; Edwards, D. G. *J. Chem. Phys.* **1950**, *18*, 127.

(14) Sengers, J. V.; Sengers, J. M. H. In "Progress in Liquid Physics"; Croxton, C. A., Ed.; Wiley: New York, 1978; p 103.

(15) Chapela, G. A.; Rowlinson, J. S. *Faraday Trans. 1* **1974**, *70*, 584.

Received for review February 28, 1983. Accepted April 9, 1983. This work has been supported by the Geothermal Division of the U.S. Department of Energy, Contract DOE EA 77-A01-6010, Task 121. Part of the research at the University of Maryland was also supported by National Science Foundation Grant DMR 8205356.